frontiers | Frontiers in Energy Research

TYPE Brief Research Report
PUBLISHED 15 September 2022
DOI 10.3389/fenrg.2022.1016536

OPEN ACCESS

EDITED BY
Xueqian Fu,
China Agricultural University, China

REVIEWED BY
Jingbo Wang,
Kunming University of Science and Technology, China
Jinlei Sun,
Nanjing University of Science and Technology, China

*CORRESPONDENCE
Xia Fang,
fangxia0709@163.com

SPECIALTY SECTION
This article was submitted to Smart Grids,
a section of the journal
Frontiers in Energy Research

RECEIVED 11 August 2022
ACCEPTED 25 August 2022
PUBLISHED 15 September 2022

CITATION
Zhang M and Fang X (2022), Bald eagle search algorithm based optimal reconfiguration of centralized Thermoelectric Generation System under non-uniform temperature distribution condition.
Front. Energy Res. 10:1016536.
doi: 10.3389/fenrg.2022.1016536

Bald eagle search algorithm based optimal reconfiguration of centralized Thermoelectric Generation System under non-uniform temperature distribution condition

Minhao Zhang and Xia Fang*

School of Mechanical Engineering, Sichuan University, Cheng Du, China

Fossil energy is becoming increasingly scarce, and technological innovation to promote clean energy consumption and achieve the "dual carbon" goal has increasingly become the focus of discussion. Compared with the full coverage thermoelectric module design scheme, the optimized layout scheme uses fewer thermoelectric generation (TEG) modules, thus confirming that the more TEG modules that are not arranged, the better. This research provides a possible way to improve the output power of TEG system. This paper proposed a bald eagle search algorithm (BES) scheme to optimize centralized TEG array reconfigures, which has not been previously employed to achieve a fast and effective tracking of the maximum power point tracking (MPPT) under non-uniform temperature difference (NTD) condition. In order to efficiently seek the global MPP (GMPP) under NTD condition, a BES algorithm is adopted to TEG reconfigures arrays to evidently improve the global searching ability of BES algorithm through the previous searching results. Furthermore, the main method in this paper is preliminarily verified on MATLAB. Both simulation and experimental results show that BES algorithm can significantly improve the convergence accuracy and output power.

KEYWORDS

maximum power point tracking, non-uniform temperature distribution, TEG array reconfiguration, bald eagle search algorithm, global maximum power point tracking

Introduction

In recent years, rapid industrial globalization and economic growth have promoted the significant growth of global power demand (Li et al., 2018). Thus far, traditional fossil energy, e.g., coal, oil, natural gases, are still the main source of power generation. The fossil energy resources are being depleted because a large part of them is needed during power generation. Besides, greenhouse gases that cause many environmental problems are produced during the process (Liu et al., 2016; Zeddini et al., 2016; Bijukumar et al., 2018; Mamura et al., 2022). In

order to address these problems, renewable energy, as a greener and sustainable alternative, attracts much attention. However, in the process of generating power by clean energy, a large amount of heat has not been effectively utilized. Therefore, using the thermoelectric effect for thermoelectric generation (TEG) to realize waste heat recovery becomes a very challenging and promising alternative (Matthew and Jae, 2015).

TEG is the method to generate power on the basis of Seebeck effect of thermoelectric materials, among which semiconductor materials are most widely utilized. One end of P-type materials and N-type materials are connected to form a P-N junction. The carrier concentration at the high-temperature end of P-N junction material is higher than that at the low-temperature end (Liu et al., 2020). The carrier begins with diffusing from the high-temperature end to the low-temperature end, forming a potential difference at the low-temperature open end. In addition, TEG has outstanding advantages such as small volume, light weight, no noise and no maintenance, high reliability and long service life (Yang et al., 2020). Therefore, TEG has been widely used in many application fields, such as solar thermoelectric power generation system, cogeneration system, energy-saving buildings, automobiles, biomass fuel hot oil heater, combined heat and power system (CHP), and so on (Zhang et al., 2019).

However, the frequent change of temperature difference leads to the unstable output power of TEG module (El-Dein et al., 2013). Therefore, it is of great essence to efficiently and accurately to adjust the optimal electrical working point in order to improve the utilization of waste heat and ensure the maximum power point tracking (MPPT) during the operation of TEG module. For example, in reference (Jian et al., 2021), a DC-DC converter adopting the incremental conductance (IC) method to realize MPPT was proposed. Compared with the MPPT method based on perturb and observe (*p*&O), MPPT based on integrated circuit has higher voltage gain and converter efficiency. Besides, reference (Ge et al., 2021) proposed a new high frequency injection (HFI) scheme, which injects high frequency signals into the system and takes the observed disturbances as feedback to control the operating conditions of TEG and reach the maximum power point (MPP).

In general, the above methods have simple structures and high reliability. However, TEG system usually operates under non-uniform temperature difference (NTD) conditions caused by incongruent heating time and distance from the heat source, in which multiple MPPs will occur (Shahbaz et al., 2020). In addition, TEG needs plenty of converters to assure a relatively high generation efficiency under NTD conditions. Therefore, compared with a string-type TEG system or modularized TEG system, a centralized TEG system only needs one converter, which can greatly reduce such converter's costs and long-term maintenance costs in the future (Sun et al., 2020). Thus, a series of MPPT strategies have been proposed to realize the MPPT of the centralized TEG system and reduce the operation costs under NTD conditions. For example, reference (Fernández-Yáñez et al., 2021) adopted a novel adaptive compass search (ACS) for MPPT of centralized TEG system under NTD condition. Compared with the original compass search (CS) relate to fixed sequence, ACS adopted an adaptive exploration direction sequence, which efficiently improved the ability to seek the global MPP (GMPP). Meanwhile, in work (Luo et al., 2021), a fast atomic search optimization (FASCO) was proposed to find the GMPP from multiple local MPPs (LMPPs). In which, in order to enhance the convergence speed and obtain high-quality solutions, the Euclidian distance ratio of original atom search optimization (ASO) was used to adaptively update according to the dynamic optimization results and the number of neighborhoods of each atom. Furthermore, a novel greedy search based data-driven (GSDD) method was designed to realize the LMPP under NTD condition (Yang et al., 2019), which adopted two-layer feedforward neural network to accurately fit the curve between power output and controllable variables according to the real-time updated operation data. Thus, based on the approximation curve, the GMPP was effectively approached from the reduced search space.

In addition, due to the huge cost of centralized TEG system control, MPPT technology is difficult to be implemented in large power plants. Due to the similarity to the optimally reconfigure PV arrays under partial shadow conditions (PSC) for real-time maximum power extraction (Chakraborty et al., 2006). Thus, the reconfiguration of the temperature difference array is considered as a satisfactory solution, which can minimize the negative impact of NTD and maximize the output power of the temperature difference array (Gavhane et al., 2017). Its basic principle is to rearrange the temperature in the same rows of temperature difference array through 1) diagonal 2) outer 3) centre and 4) random to balance the impact of NTD (Zhang et al., 2022). Inspired by the reconfiguration of PV arrays (Fathy, 2018; Fathy, 2020; Lamzouri et al., 2020), this paper proposes a novelist bald eagle search algorithm (BES) for the reconfiguration of TEG arrays to improve power generation efficiency.

The rest of this paper is as follows: Section 2 introduces the physical model and mathematical model of TEG; Section 3 introduces the mechanism and principle of the BES algorithm, and describes the fitness function and constraints of the temperature difference reconstruction based on the BES algorithm. In Section 4, the superiority of the BES algorithm is proved by comparing the optimization results of the BES algorithm with the GA algorithm. Finally, Section 5 provides several practical conclusions and prospects for future research.

2 Thermoelectric generation system modeling

2.1 Modelling of thermoelectric generation module

2.1.1 Physical modelling of thermoelectric generation module

TEG is a solid-state device that makes use of cold and hot temperature difference convection to generate power on the

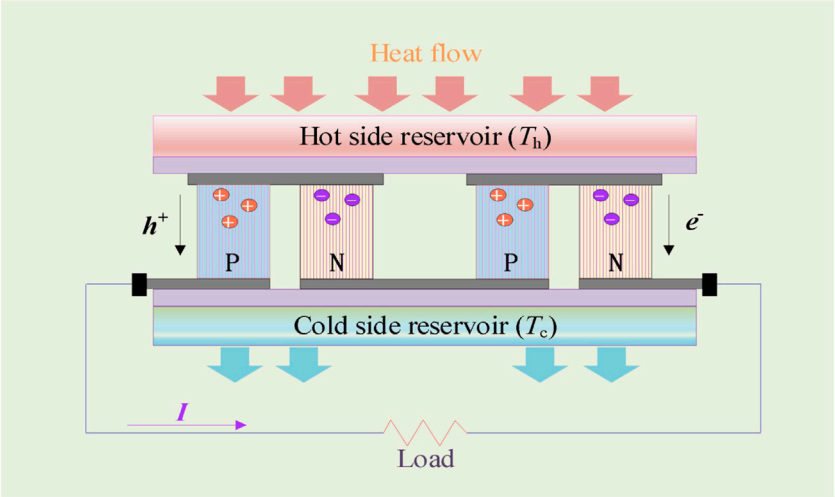

FIGURE 1
Physical model of a TEG module.

basis of Seebeck effect. Generally, it consists of a group of small thermoelectric modules where two semiconductor pins (one doped *p* and one doped N) are electrically connected in series and thermally in parallel. The interior is divided into cold and hot pole where thermal energy is supplied at hot pole and thermal energy not converted into electric energy is output at the cold pole. The typical physical model of TEG module is shown in Figure 1 When one end of the device is in a high temperature state and the other end is in a low temperature state, electromotive force will be formed in the circuit. Generally, in the application of thermoelectric power generation, multiple PN junctions are connected in series to form a thermoelectric conversion module (Hasanien et al., 2016; Yousri et al., 2022).

2.1.2 Mathematical modelling of thermoelectric generation module

On the basic of Figure 1, the equivalent TEG module circuit indicates that TEG module can be modelled as a voltage source connected in series with an internal resistor. The values of voltage source and resistance vary with temperature, the mathematical relation between voltage source and temperature can be describe as

$$\varepsilon = \alpha_s (T_h - T_c) = \alpha_s \Delta T \tag{1}$$

where T_h andT_c denote the temperature of the hot and cold hole of TEG, respectively; α_s called Seebeck coefficient reflects the Seebeck effect of the material, the mathematical relationship between α_s and temperature can be expressed as

$$\alpha_s (T) = \alpha_0 + \alpha_1 \ln (T/T_0) \tag{2}$$

where α_0 represents the fundamental portion of Seebeck coefficient; α_1 is the variation rate of Seebeck coefficient;T and T_0 denotes the even temperature and the temperature reference, respectively.

When TEG module is connected to load R_L, the current flowing the circuit and the corresponding generated power output power can be written as

$$I = \frac{\varepsilon}{R_L + R_{TEG}} \tag{3}$$

$$P = \left(\frac{\varepsilon}{R_L + R_{TEG}}\right)^2 R_L \tag{4}$$

where R_L represents the load connected to TEG; R_{TEG} is the equivalent internal resistance of a TEG module.

2.2 Modelling of thermoelectric generation system

TEG system connects TEG modules in series and parallel configurations to generate desired output power. A $M \times N$ topology of TEG array is shown in Figure 2 indicates the equivalent circuit of individual TEG module and the column of TEG array. The open-circuit voltage and internal resistance of TEG module in row i, column j is represented as ε_{ij} and R_{TEG_ij} $(i = 1, \ldots, n; j = 1, \ldots, n)$, likewise, the open circuit voltage and internal resistance of the j column of TEG array are represented as ε_j and R_{TEG_j}, respectively.

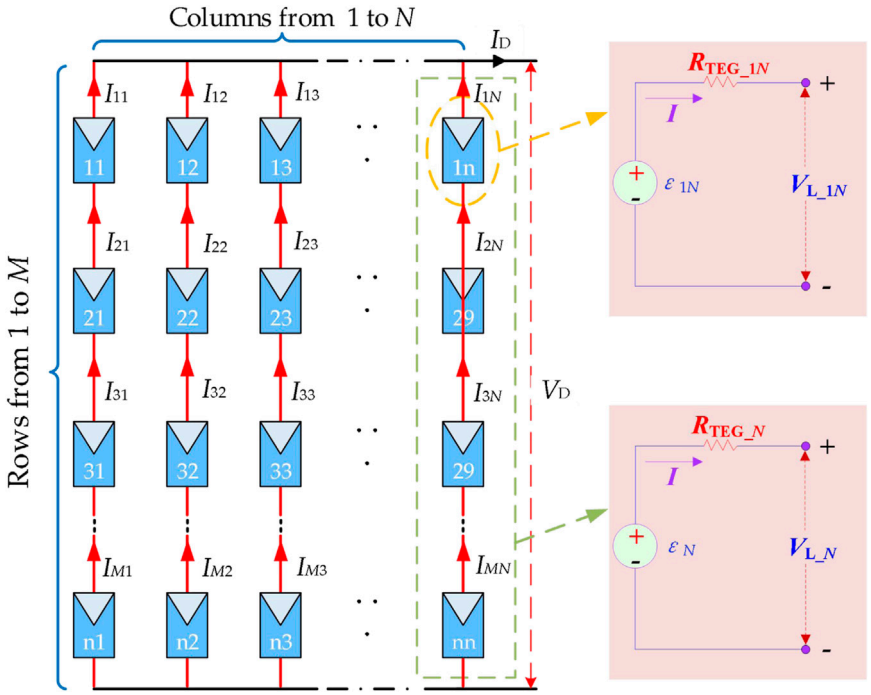

FIGURE 2
Topology of M × N circuit of TEG system.

The relationship between the equivalent circuit of individual TEG module and the equivalent circuit of the corresponding column of TEG array can be described as

$$\varepsilon_j = \sum_{i=1}^{n} \varepsilon_{ij} \tag{5}$$

$$R_{TEG\_j} = \sum_{i=1}^{n} R_{TEG\_ij} \tag{6}$$

The output current of TEG system, I_o can be given as Eq. 7. Likewise, the output voltage V_o of TEG system can be described as Eq. 8.

$$I_o = \sum_{j=1}^{n} I_{ij} \, (i = 1, 2, \ldots, n) \tag{7}$$

$$V_o = \sum_{i=1}^{n} \varepsilon_{ij} \, (j = 1, 2, \ldots, n) \tag{8}$$

Therefore, the output power P_o of TEG system can be derived from I_o and V_o as Eq. 9.

$$P_o = I_o \times V_o \tag{9}$$

Furthermore, the substitution of temperature into Eq. 9 to indicate the relationship between temperature and P_o can be obtained as Eq. 10.

$$P_o = \frac{R_{LS} \left\{ \sum_{j=1}^{n} \sum_{i=1}^{n} \frac{\left[\alpha_0 + \alpha_1 \ln\left(\frac{T_{ij}}{T_0}\right) \right] \left(T_{h\_ij} - T_{c\_ij} \right)}{R_{TEG\_j}} \right\}^2}{\left(1 + \sum_{j=1}^{n} \frac{R_{LS}}{R_{TEG\_j}} \right)^2} \tag{10}$$

where R_{LS} denotes the load connected to TEG system.

3 Design of bald eagle search for thermoelectric generation arrays reconfiguration

3.1 Principles of bald eagle search algorithm

3.1.1 Selecting the search space

The bald eagle randomly selects the search area, and determines the best search position by judging the number of prey, which is convenient for searching for the prey. At this stage, the bald eagle position P_i, new update is determined by multiplying the prior information of random search by α. The mathematical model of this behavior is described as

$$P_{i,new} = P_{best} + \alpha \times \gamma (P_{mean} + P_i) \tag{11}$$

where α represents the control position variation parameter, the variation range is (1.5, 2); y is a random number between (0, 1); P_{best} is the best search position determined by the current vulture search; P_{mean} is the average distribution position of bald eagles after the previous search; P_i is the position of the ith bald eagle (Krishnan et al., 2020).

3.1.2 Search space prey

The bald eagle flies in a spiral shape in the selected search space to search for prey, accelerate the search process, and find the best dive capture position. The mathematical model of the spiral flight uses the polar coordinate equation to update the position as follows:

$$\theta(i) = a \times \pi \times rand \tag{12}$$

$$r(i) = \theta(i) + R \times rand \tag{13}$$

$$xr(i) = r(i) \times sin(\theta(i)),\ yr(i) = r(i) \times cos(\theta(i)) \tag{14}$$

$$x(i) = \frac{xr(i)}{max\ (|xr|)},\quad y(i) = \frac{yr(i)}{max\ (|yr|)} \tag{15}$$

where $\theta(i)$ and $r(i)$ are the polar angle and polar diameter of the spiral equation, respectively; ? and ? are the parameters that control the spiral trajectory, and the variation ranges are (0, 5) and (0.5, 2) respectively; rand is (0, 1) random numbers, $x(i)$ and $y(i)$ represent the position of the bald eagle in polar coordinates, and the values are (-1, 1). The position of the bald eagle is updated as follows:

$$P_{i,new} = rand \times P_{best} + x_1(i) \times (P_i - c_1 \times P_{mean}) + y_1(i) \times (P_i - c_2 \times P_{best}) \tag{16}$$

where $P_{i,new}$ is the next update position of the ith bald eagle.

3.1.3 Diving to capture prey

The bald eagle quickly dives from the optimal position in the search space to fly to the target prey, and other individuals of the population also move to the optimal position and attack the prey at the same time. The motion state is still described by the polar coordinate equation, as follows:

$$\theta(i) = a \times \pi \times rand,\quad r(i) = \theta(i) \tag{17}$$

$$xr(i) = r(i) \times sinh\ [\theta(i)],\quad yr(i) = r(i) \times cosh\ [\theta(i)] \tag{18}$$

$$x_1(i) = \frac{xr(i)}{max\ (|xr|)},\quad y_1(i) = \frac{yr(i)}{max\ (|yr|)} \tag{19}$$

The update formula for the position of the bald eagle in the dive is:

$$\begin{cases} \delta_x = x_1(i) \times (P_i - c_1 \times P_{mean}) \\ \delta_y = y_1(i) \times (P_i - c_2 \times P_{best}) \end{cases} \tag{20}$$

$$P_{i,new} = rand \times P_{best} + \delta_x + \delta_y \tag{21}$$

where c_1 and c_2 represent the movement intensity of the bald eagle to the optimal and central position, and the values are (1, 2).

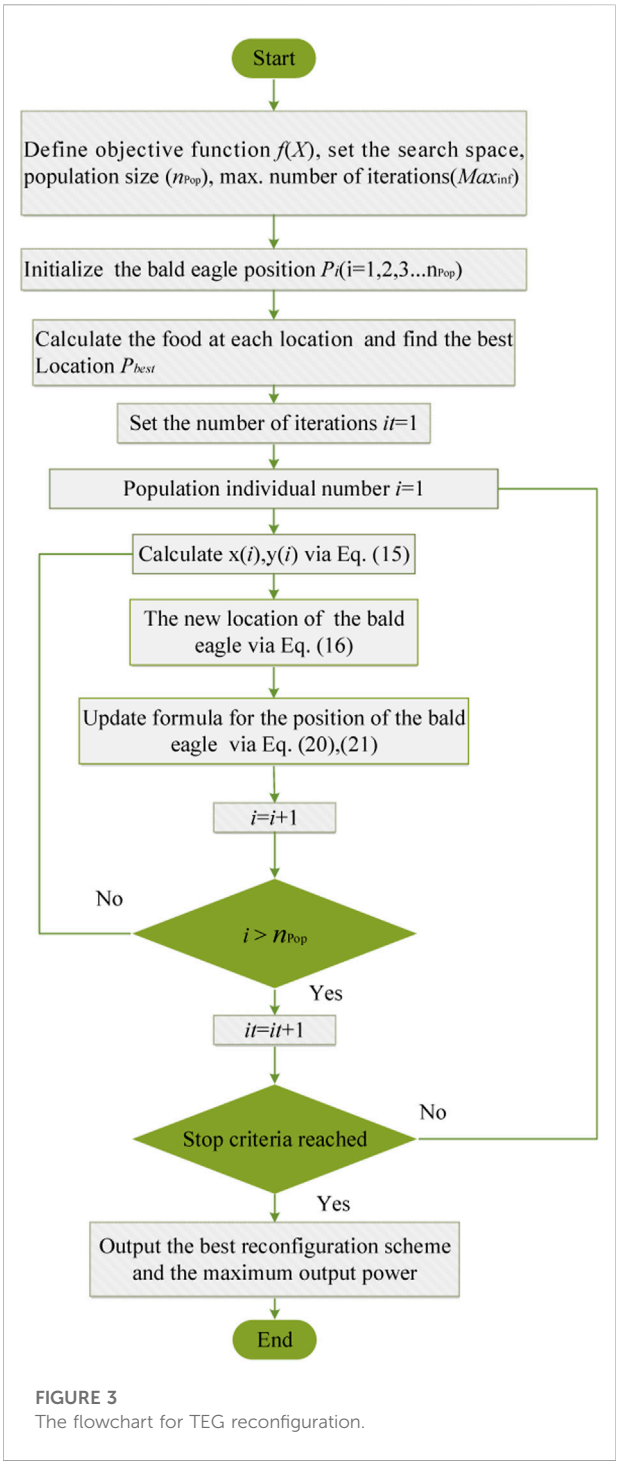

FIGURE 3
The flowchart for TEG reconfiguration.

3.2 Bald eagle search algorithm design for thermoelectric generation reconfiguration

3.2.1 Fitness function

Since the output power generated by each TEG module is constant. In particularly, the operating point may deviate from

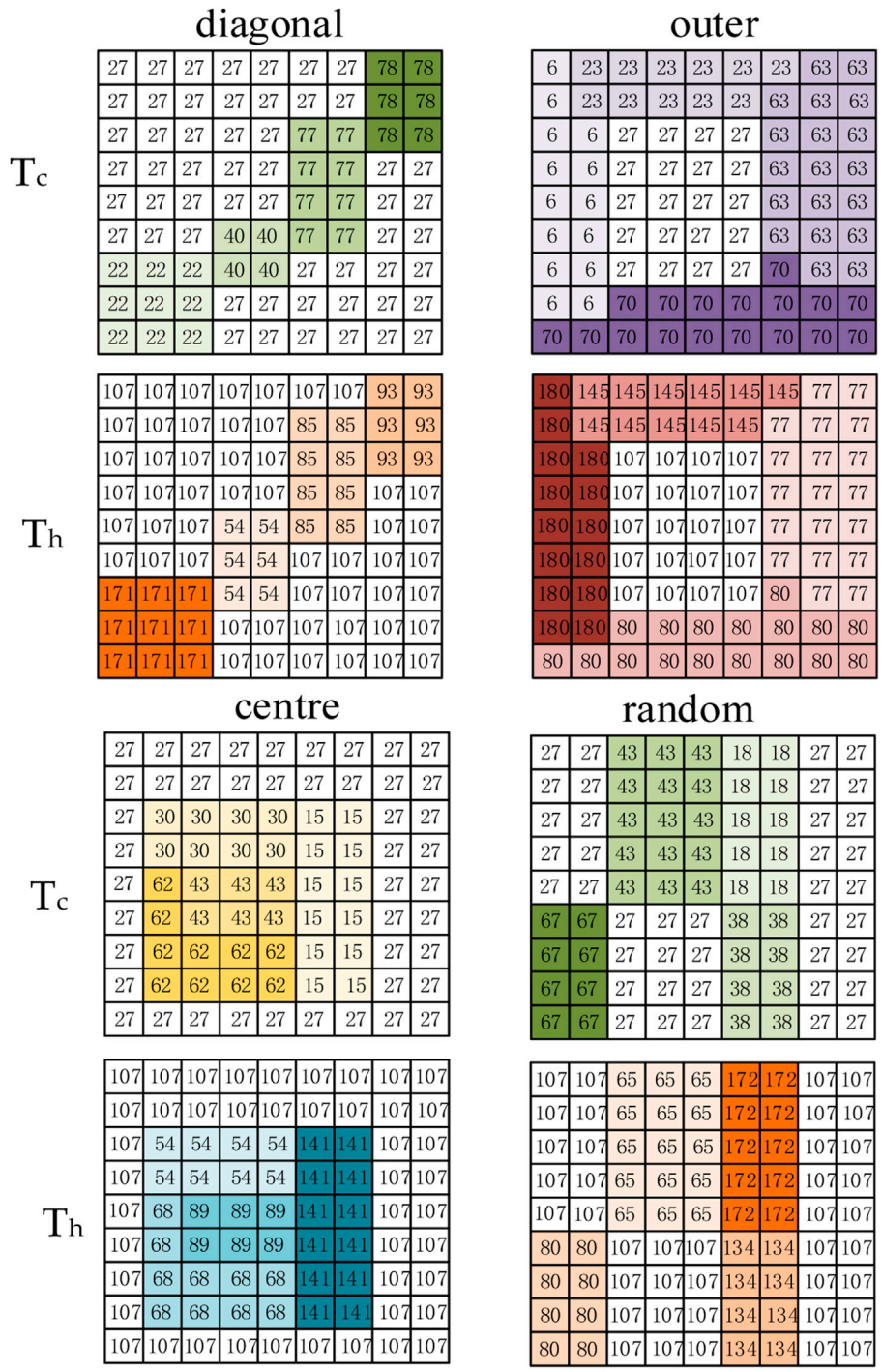

FIGURE 4
Four NTD patterns in the 9 × 9 symmetric TEG array.

the maximum power point, such as when parallel TEG module operates under NTD conditions. However, the result is a sharp drop in output power. Therefore, in order to improve the output power of the TEG module and reduce the mismatch loss, it can be improved by reconfiguring the temperature of the TEG array. The maximum output power (F_{max}) as follows:

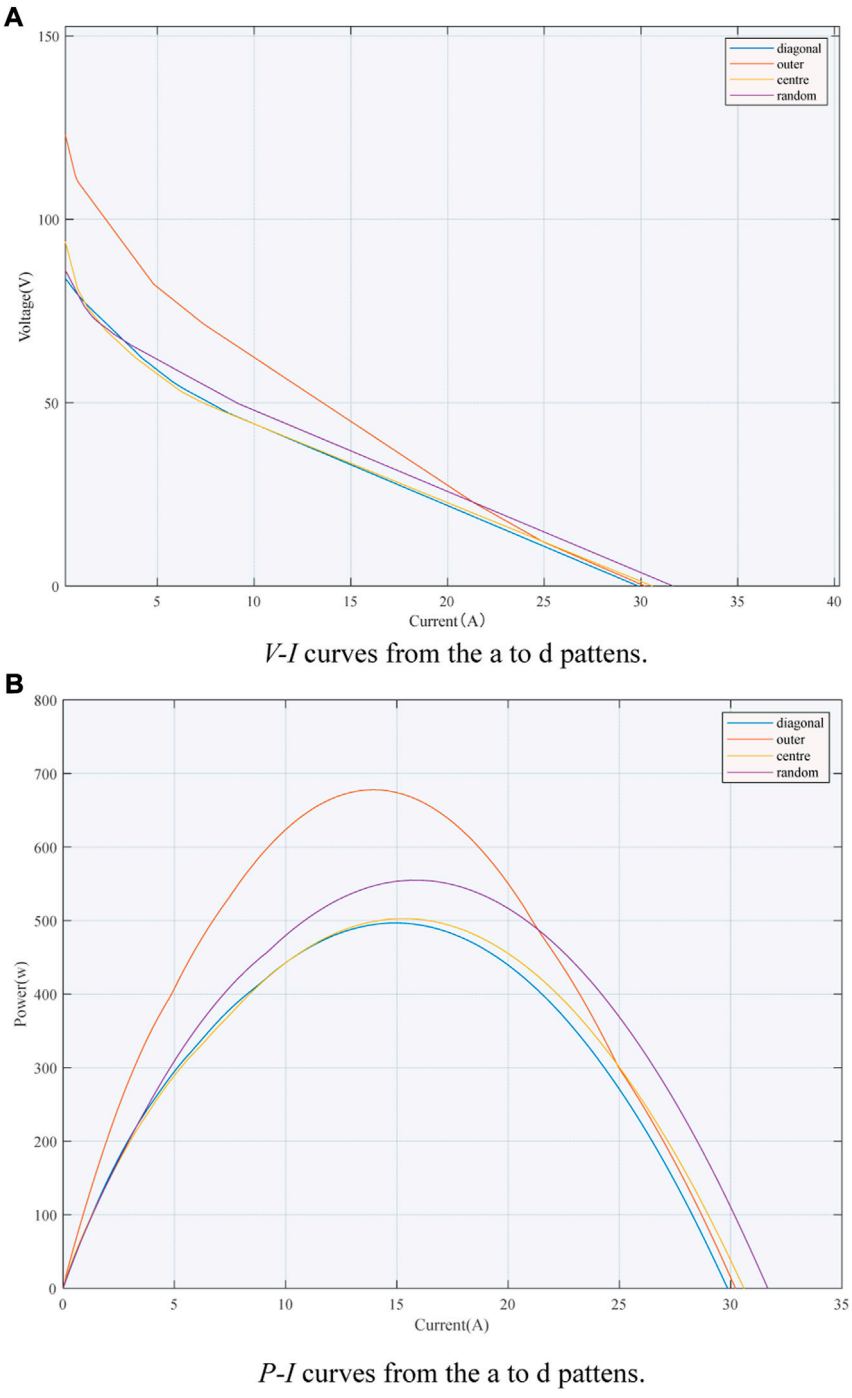

FIGURE 5
Output characteristics curves of a 9 × 9 symmetric TEG array. **(A)** *V-I* curve. **(B)** *P-I* curve.

$$F_{max} = max\left(\sum_{h=1}^{N} V_h \times I_h\right) \tag{22}$$

where I_h and V_h are the current and voltage of the *hth* column.

3.2.2 Constraint condition

The refactoring principle of TEG is that TEG arrays are only swapped with other arrays in the same row. In addition, reconfigurable variables should satisfy the following conditions.

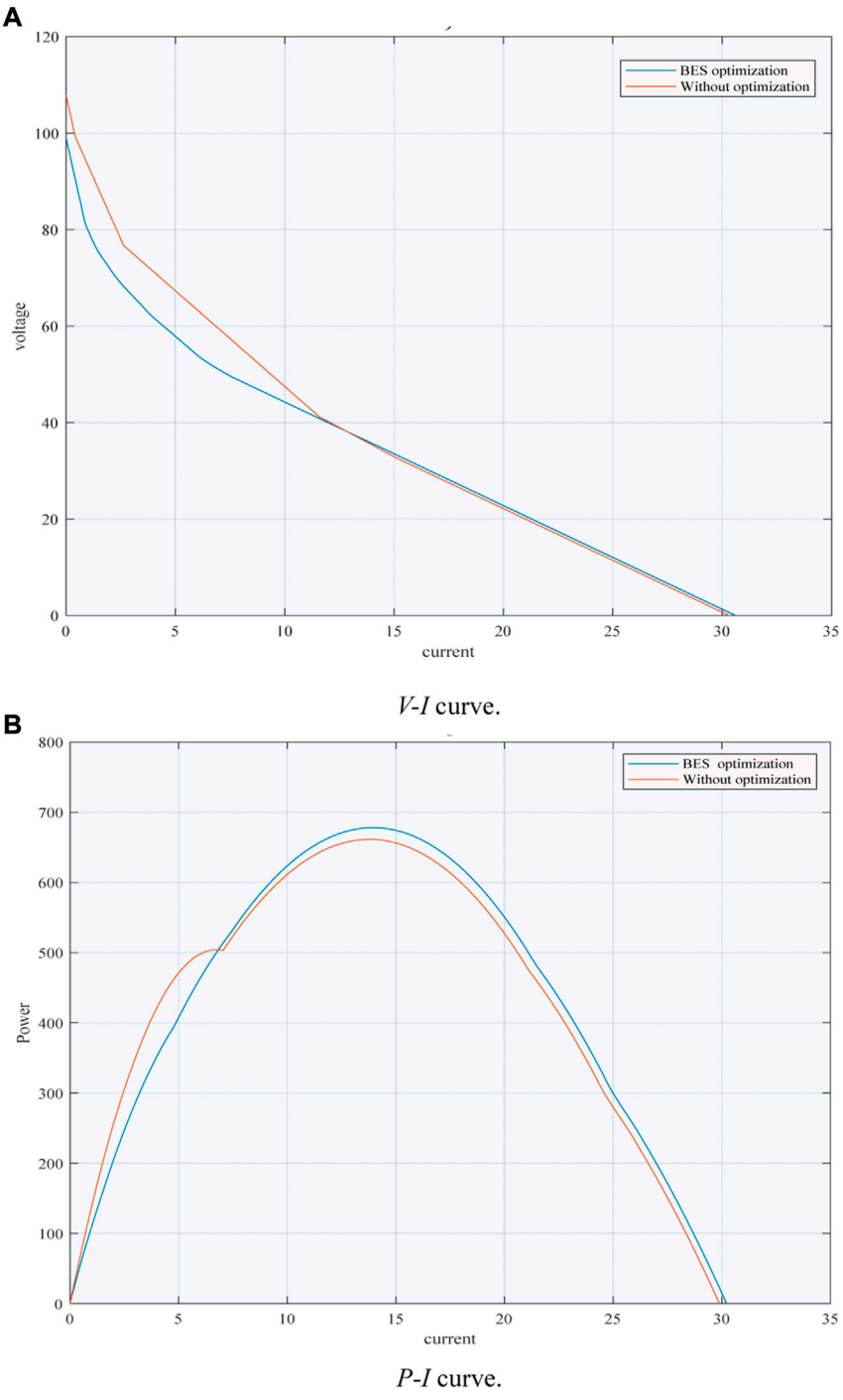

FIGURE 6
The *V-I* and *P-I* curves with and without the optimization. **(A)** *V-I* curve. **(B)** *P-I* curve.

$$k_{ij} \in \{1, 2, \cdots, N\}, i = 1, 2, 3, \ldots, M; j = 1, 2, 3, \ldots, N \quad (23)$$

where k_{ij} represents the electrical switch state of the *ith* row and the *jth* column arrays.

3.2.3 Execution process

The corresponding schematic flowchart is demonstrated Figure 3.

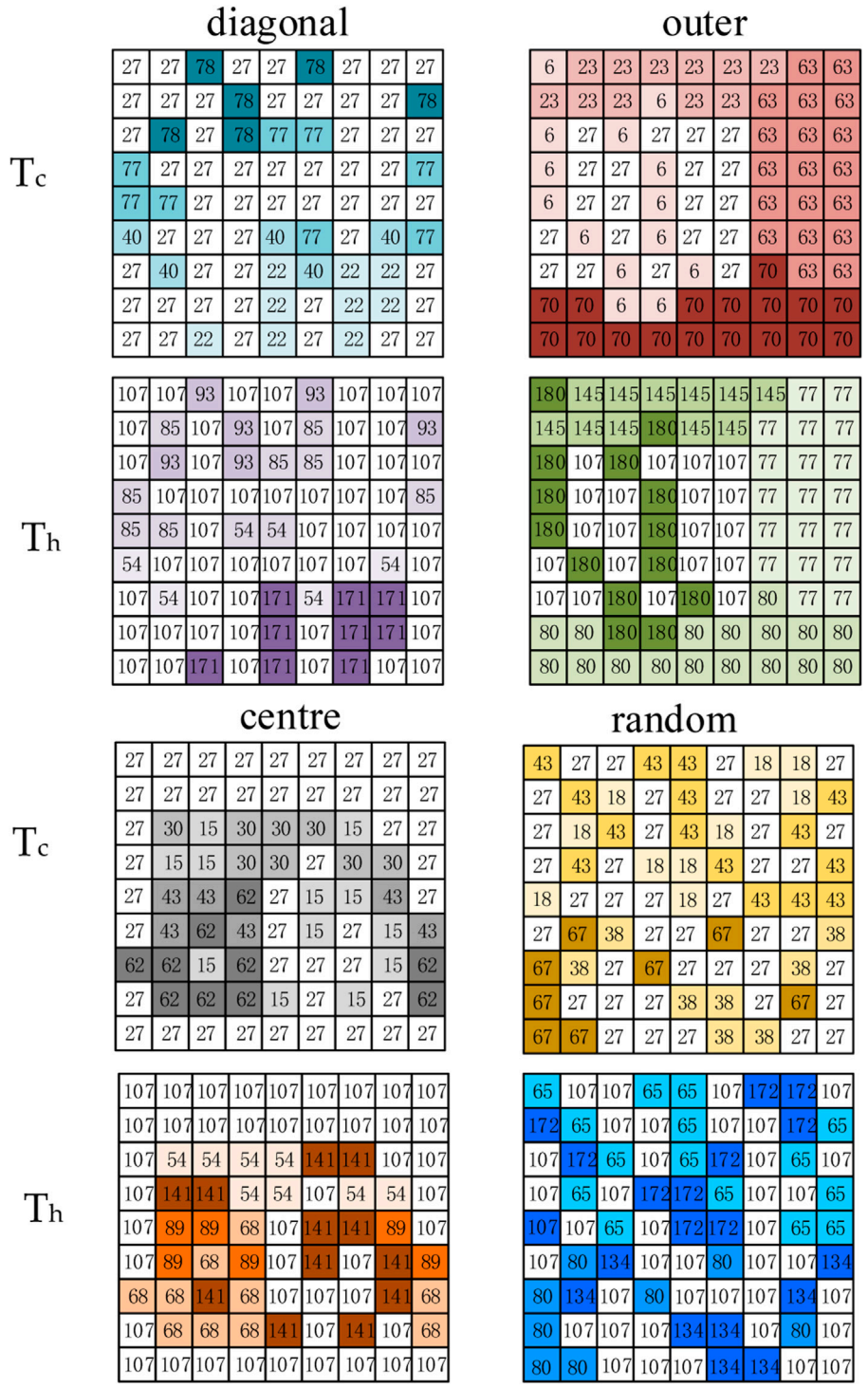

FIGURE 7
Four NTD patterns in the 9 × 9 symmetric TEG array after reconfiguration.

TABLE 1 Output optimal power obtained by BES algorithm under HTD conditions.

NTD Pattern	p'_{out}(W)	BES				GA			
		P_{max}(W)	P_{min} (W)	P_{avg} (W)	STD	P_{max} (W)	P_{min}(W)	P_{avg}(W)	STD
Diagonal	627.3379	634.92	610.2	605.76	0.2005	557.08	540.36	543.72	0.7815
Outer	600.5703	665.32	553.16	593.88	0.6154	679.00	671	671.52	0.702
Centre	625.0512	631.96	630.44	631.2	0.3680	632.08	631.8	631.72	0.1966
Random	590.2325	604.72	582.76	587.96	0.5615	618.00	592.32	592.80	0.119

4 Case studies

The array reconfiguration was carried out for six different HTD patterns (i.e., 1) diagonal 2) outer 3) centre and 4) random for a TEG array with a 9 × 9 topology. Furthermore, the results were derived from the optimization of BES algorithm, which were compared with the results without reconfiguration. In addition, the maximum number of iterations K, the population size Pop as well as the number of independent runs N_{run} were set at 30, 40, and 50, respectively. All the simulations were executed on MATLAB/Simulink 2019b *via* a personal computer with an IntelR CoreTM i5 CPU at 2.9 GHz and 16 GB of RAM.

4 1 9 × 9 symmetric thermoelectric generation array

This section provides a comprehensive and holistic comparison of the reconfiguration optimization of BES algorithm in the four temperature modes with the unreconfigured output power. In particular, the four NTD distributions in a 9 × 9 symmetric TEG array are shown Figure 4, where the numbers on each block represent the temperature of the module, and different colors represent different temperatures Figure 5 shows the *V-I* and *P-I* curves of a 9 × 9 symmetric TEG array after reconfiguration. Among them, especially under the conditions of random temperature difference and central temperature difference, the maximum output power obtained by BES algorithm after reconstruction and optimization is 26.05 and 15.96% higher than the maximum output power obtained without reconstruction and optimization. In addition, as shown Figure 6, after the optimization of BES algorithm, the multi-peak phenomenon disappears Figure 7 shows the 9 × 9 symmetrical distribution of high and low temperature TEG arrays for each NTD condition after reconfiguration based on BES algorithm.

In addition, P_{max}, P_{min}, P_{avg}, and STD in Table 1 are the maximum, minimum, average and standard deviation of the output power in 20 independent runs. This has a certain reference value for evaluating the reliability and standard deviation of TEG arrays using the BES algorithm. It can be seen that the optimization performance of the BES algorithm is obvious, and the maximum output power of the TEG system is improved. In the four NTD modes (for example, 1) diagonal 2) outer 3) centre and 4) random), the power enhancement values of the maximum power are 7.113, 2.558, 4.030, and 6.778%, respectively. In summary, BES algorithm can be closer to GMPP through population search. Through a simple optimization mechanism and a single search rule, the reconstruction power of the TEG array can be significantly improved, and the power loss can be effectively reduced.

5 Conclusions

This paper designs an innovative reconfiguration technology based on bald eagle search algorithm for centralized TEG system under NTD condition, which main findings/contributions can be drawn as follows:

1) A technology of centralized TEG system reconfiguration optimization is proposed for the first time, which is similar to PV reconfiguration, to improve maximum power and make the *P-I* characteristic curve return to single peak. The paper proposed a bald eagle search algorithm to optimize centralized TEG system reconfigures arrays, which has not been previously employed to achieve a fast and effective tracking of the MPPT under NTD conditions;
2) Compared with GA algorithms, The algorithm has strong global search ability and can effectively solve various complex numerical optimization problems, which also adopts a more prominent exploration search for approximating the GMPP of centralized TEG system reconfigures arrays under NTD conditions. Therefore, it can obtain a high-quality GMPP with a higher speed and convergence stability than GA algorithms;
3) BES algorithm based MPPT technique is developed for centralized TEG system reconfigures arrays that owns the lowest costs of converter maintenance, and the wasted heat can be efficiently reused and recycled during the industrial process. This paper comprehensively considers the impact caused under NTD conditions and simulates the actual temperature distribution including two types of wasted heat. Besides, a design of

electrical switching arrangement is performed for 9 × 9 symmetric TEG arrays so that it can easily deal with any NTD conditions.

Finally, compared with GA algorithms, a bald eagle search algorithm is also a model-free algorithm, which is highly independent of the specific mathematical model of the optimization problem. Hence, it has high application flexibility and can be employed to other optimization problems of energy conversion, such as MPPT of PV systems.

Data availability statement

The raw data supporting the conclusions of this article will be made available by the authors, without undue reservation.

Author contributions

MZ: Conceptualization, Writing-Reviewing and Editing, Supervision; XF: Writing-Original draft preparation, Investigation, Resources.

Funding

The authors gratefully acknowledge the support of Key R&D project of Sichuan Science and Technology Planning Project (2022YFG0058).

Conflict of interest

The authors declare that the research was conducted in the absence of any commercial or financial relationships that could be construed as a potential conflict of interest.

Publisher's note

All claims expressed in this article are solely those of the authors and do not necessarily represent those of their affiliated organizations, or those of the publisher, the editors and the reviewers. Any product that may be evaluated in this article, or claim that may be made by its manufacturer, is not guaranteed or endorsed by the publisher.

References

Bijukumar, B., Raam, A. G.K., Ilango, G.S., and Nagamani, C. (2018). A linear extrapolation based MPPT algorithm for thermoelectric generators under dynamically varying temperature conditions. *IEEE Trans. Energy Convers.* 33 (4), 1641–1649. doi:10.1109/TEC.2018.2830796

Chakraborty, A., Saha, B.B., Koyama, S., and Ng, K.C. (2006). Thermodynamic modelling of a solid state thermoelectric cooling device: Temperature-entropy analysis. *Int. J. Heat Mass Transf.* 49, 3547–3554. doi:10.1016/j.ijheatmasstransfer.2006.02.047

El-Dein, M. Z.S., Kazerani, M., and Salama, M. M. A. (2013). Optimal photovoltaic array reconfiguration to reduce partial shading losses. *IEEE Trans. Sustain. Energy* 4 (1), 145–153. doi:10.1109/TSTE.2012.2208128

Fathy, A. (2020). Butterfly optimization algorithm based methodology for enhancing the shaded photovoltaic array extracted power via reconfiguration process. *Energy Convers. Manag.* 220, 113115. doi:10.1016/j.enconman.2020.113115

Fathy, A. (2018). Recent meta-heuristic grasshopper optimization algorithm for optimal reconfiguration of partially shaded PV array. *Sol. Energy* 171, 638–651. doi:10.1016/j.solener.2018.07.014

Fernández-Yáñez, P., Romero, V., Armas, O., and Cerretti, G. (2021). Thermal management of thermoelectric generators for waste energy recovery. *Appl. Therm. Eng.* 196, 117291. doi:10.1016/j.applthermaleng.2021.117291

Gavhane, P.S., Krishnamurthy, S., Dixit, R., Ram, J. P., and Rajasekar, N. (2017). EL-PSO based MPPT for solar PV under partial shaded condition. *Energy Procedia* 117, 1047–1053. doi:10.1016/j.egypro.2017.05.227

Ge, M.H., Li, Z.H., Wang, Y.T., Zhao, Y., Zhu, Y., Wang, S., et al. (2021). Experimental study on thermoelectric power generation based on cryogenic liquid cold energy. *Energy* 220, 119746. doi:10.1016/j.energy.2020.119746

Hasanien, H.M., Al-Durra, A., and Muyeen, S.M. (2016) "Gravitational search algorithm-based PV array reconfiguration for partial shading losses reduction," in 5th IET International Conference on Renewable Power Generation (RPG), London, UK, 21-23 Sept. 2016, 703–708. doi:10.1049/cp.2016.0577

Jian, L., Zhen, Y., Li, H., Hu, S., Duan, Y., and Yan, J. (2021). Optimal schemes and benefits of recovering waste heat from data center for district heating by CO2 transcritical heat pumps. *Energy Convers. Manag.* 245, 114591. doi:10.1016/j.enconman.2021.114591

Krishnan, S., Kinattingal, S.G., Simon, S.P., and Nayak, P. S. R. (2020). MPPT in PV systems using ant colony optimisation with dwindling population. *IET Renew. Power Gener.* 14 (7), 1105–1112. doi:10.1049/iet-rpg.2019.0875

Lamzouri, F-E., Boufounas, E-M., Brahmi, A., and Amrani, A. E. (2020). Optimized TSMC control based MPPT for PV system under variable atmospheric conditions using PSO algorithm. *Procedia Comput. Sci.* 170, 887–892. doi:10.1016/j.procs.2020.03.116

Li, X. S., Wen, H. Q., Hu, Y. H., and Jiang, L. (2018). A novel beta parameter based fuzzy-logic controller for photovoltaic MPPT application. *Renew. Energy* 130, 416–427. doi:10.1016/j.renene.2018.06.071

Liu, J., Yao, W., Wen, J.Y., Fang, J., Jiang, L., He, H., et al. (2020). Impact of power grid strength and PLL parameters on stability of grid-connected DFIG wind farm. *IEEE Trans. Sustain. Energy* 11 (1), 545–557. doi:10.1109/TSTE.2019.2897596

Liu, Y.H., Chiu, Y.H., Huang, J.W., and Wang, S.C. (2016). A novel maximum power point tracker for thermoelectric generation system. *Renew. Energy* 97, 306–318. doi:10.1016/j.renene.2016.05.001

Luo, D., Wang, R., Yan, Y., Yu, W., and Zhou, W. (2021). Transient numerical modelling of a thermoelectric generator system used for automotive exhaust waste heat recovery. *Appl. Energy* 297, 117151. doi:10.1016/j.apenergy.2021.117151

Mamura, H, Üstünera, M.A, and AminBhuiyanb, L.R (2022). Future perspective and current situation of maximum power point tracking methods in thermoelectric generators. *Sustain. Energy Technol. Assessments* 50, 101824. doi:10.1016/j.seta.2021.101824

Matthew, B., and Jae, D.P. (2015). Current-sensorless power estimation and MPPT implementation for thermoelectric generators. *IEEE Trans. Ind. Electron.* 62 (9), 5539–5548. doi:10.1109/TIE.2015.2414393

Shahbaz, M., Raghutla, C., Chittedi, K.R., Jiao, Z., and Vo, X. V. (2020). The effect of renewable energy consumption on economic growth: Evidence from the renewable energy country attractive index. *Energy* 207, 118162. doi:10.1016/j.energy.2020.118162

Sun, K., Yao, W., Fang, J.K., Ai, X., Wen, J., and Cheng, S. (2020). Impedance modeling and stability analysis of grid-connected DFIG-based wind farm with a VSC-HVDC. *IEEE J. Emerg. Sel. Top. Power Electron.* 8 (2), 1375–1390. doi:10.1109/JESTPE.2019.2901747

Yang, B., Wang, J.B., Zhang, X.S., Yu, T., Yao, W., Shu, H., et al. (2020). Comprehensive overview of meta-heuristic algorithm applications on PV cell parameter identification. *Energy Convers. Manag.* 208, 112595. doi:10.1016/j.enconman.2020.112595

Yang, B., Wang, J.T., Zhang, X.S., Zhang, M., Shu, H., Li, S., et al. (2019). MPPT design of centralized thermoelectric generation system using adaptive compass search under non-uniform temperature distribution condition. *Energy Convers. Manag.* 199, 111991. doi:10.1016/j.enconman.2019.111991

Yousri, D., Babu, T.S., Mirjalili, S., Rajasekar, N., and Elaziz, M. A. (2022). A novel objective function with artificial ecosystem-based optimization for relieving the mismatching power loss of large-scale photovoltaic array. *Energy Convers. Manag.* 225, 113385. doi:10.1016/j.enconman.2020.113385

Zeddini, M.A., Pusca, R., Sakly, A., and Mimouni, M. F. (2016). PSO-based MPPT control of wind-driven Self-excited induction generator for pumping system. *Renew. Energy* 95, 162–177. doi:10.1016/j.renene.2016.04.008

Zhang, H.X., Lu, Z.X., Hu, W., Wang, Y., Dong, L., and Zhang, J. (2019). Coordinated optimal operation of hydro-wind-solar integrated systems. *Appl. Energy* 242, 883–896. doi:10.1016/j.apenergy.2019.03.064

Zhang, R., Yang, B., and Chen, N. (2022). Arithmetic optimization algorithm based MPPT technique for centralized TEG systems under different temperature gradients. *Energy Rep.* 8, 2424–2433. doi:10.1016/j.egyr.2022.01.185